# Model-to-Data Comparisons Reveal Influence of Jellyfish Interactions on Plankton Community Dynamics

Kevin P. Crum
*Rutgers - The State University of New Jersey, Newark*

Heidi L. Fuchs
*Rutgers - The State University of New Jersey, New Brunswick*

Paul Bologna
*Montclair State University*, bolognap@montclair.edu

John Gaynor
*Montclair State University*, gaynorj@mail.montclair.edu

Model-to-data comparisons reveal influence of jellyfish interactions on plankton community dynamics

Author(s): Kevin P. Crum, Heidi L. Fuchs, Paul A. X. Bologna and John J. Gaynor

## REFERENCES

JSTOR

# Model-to-data comparisons reveal influence of jellyfish interactions on plankton community dynamics

**Kevin P. Crum[1], Heidi L. Fuchs[1],\*, Paul A. X. Bologna[2], John J. Gaynor[2]**

[1]Institute of Marine and Coastal Science, Rutgers University, New Brunswick, NJ 08901, USA
[2]Montclair State University, Montclair, NJ 07043, USA

ABSTRACT: Taxonomic shifts can alter predator feeding preference and modify ecosystem dynamics through top-down control. In Barnegat Bay–Little Egg Harbor Estuary (New Jersey, USA), sea nettle *Chrysaora quinquecirrha* abundances have increased in the northern portions of the estuary. We evaluated the geographical variation in top-down influence of *C. quinquecirrha* on plankton community dynamics. We simulated a range of jellyfish- to copepod-dominated eco-systems using a size-resolved nutrient–phytoplankton–zooplankton (NPZ) model. Zooplankton feeding was parameterized as a community average based on predator–prey size ratios and breadth of prey sizes of dominant species. We compared model outputs to data collected in the estuary during 2 summer months of high *C. quinquecirrha* abundance. We predicted that data from the northern region would be more similar to the jellyfish-dominated model outputs, because *C. quinquecirrha* abundance is higher in the north. Contrary to expectations, all northern sites had observational data more similar to the copepod-dominated model outputs, and the site that was most similar to the jellyfish-dominated model outputs was in the *C. quinquecirrha*-free southern region. These results may indicate complex interactions between *C. quinquecirrha* and the ctenophore *Mnemiopsis leidyi*, a voracious copepod predator that is nearly absent in the northern region despite having wide environmental tolerances. Predation by *C. quinquecirrha* may limit the distribution of *M. leidyi* and indirectly strengthen copepod dominance in the northern region of the estuary. These results suggest that top-down control by jellyfish can be strongly influenced by competition among gelatinous taxa.

KEY WORDS: Size-structured model · Top-down control · Prey size preference · Zooplankton · Ctenophore · *Mnemiopsis leidyi* · Atlantic sea nettle · *Chrysaora quinquecirrha* · Copepod

*—————— Resale or republication not permitted without written consent of the publisher ——————*

## INTRODUCTION

Top-down control is a process whereby organisms influence the trophic structure and abundance of organisms at lower trophic levels through predation. Although top-down control is strong enough in some systems to produce trophic cascades (Estes et al. 1998, Frank et al. 2005), such dramatic effects are uncommon in mid- to low-latitude marine plankton communities (Sommer 2008). Copepods are the main herbivores in these communities and prey heavily on large phytoplankton cells. Blooms of copepods can initially decrease total phytoplankton biomass, but growth of less-grazed phytoplankton size classes will eventually recoup the losses in total phytoplankton biomass (Sommer 2008). Therefore, marine planktonic perturbations often lead to shifts in abundance rather than trophic cascades. Top-down control in marine plankton communities is strongly related to feeding selectivity of predators.

Predator feeding selectivity is determined by factors ranging from predator anatomy and behavior to prey density and biochemical composition. The feeding apparatus sets the absolute limits on the prey sizes that a predator is able to consume (Hansen et al. 1994). Within that range, clearance and uptake rates of prey are influenced by prey motility (González et al. 1993), concentration (Bogdan & Gilbert 1982), and biochemical composition (Poulet & Marsot 1978). Feeding selectivity is further refined by the predator's feeding mode (e.g. filter feeder or raptorial feeder; Hansen et al. 1994).

Many of the complexities in predator feeding selectivity can be generalized based on organism size. The feeding preference of a predator of a given size is defined by the predator–prey size ratio and the range of prey sizes on which it can feed, with generalists feeding on a wide range of prey sizes and specialists feeding on a narrower range of prey sizes. Predators tend to feed optimally on prey smaller than themselves (Hansen et al. 1994, Barnes et al. 2010). Ingestion rate of prey decreases when prey size is further from optimal. The optimal prey size scales with predator size, leading to consistent predator–prey size ratios within taxonomic groups (Hansen et al. 1994). However, the optimal predator–prey size ratio can vary greatly among and within taxa (Hansen et al. 1994, Fuchs & Franks 2010). Predator–prey size ratios tend to be lowest among dinoflagellates, highest among salps, and intermediate among other groups (Fuchs & Franks 2010).

In modeling studies, zooplankton feeding preferences influence marine community structure and dynamics through top-down control. Altering the zooplankton functional response causes shifts in phytoplankton distributions in a spatially resolved ecosystem model (Anderson et al. 2010) and changes phytoplankton diversity in a global ecosystem model (Prowe et al. 2012). In size-resolved nutrient–phytoplankton–zooplankton (NPZ) models, ecosystem biomass (Banas 2011) and phytoplankton biomass (Fuchs & Franks 2010) respond less predictably to nutrient forcing in communities with more generalist feeding than in communities with more specialist feeding. Simulated plankton communities tend to have higher connectance and steeper size spectra when zooplankton feed on prey much smaller than themselves (Fuchs & Franks 2010). Recent studies have parameterized zooplankton feeding selectivity using morphometric ratios (Wirtz 2012) and optimal foraging (Visser & Fiksen 2013). Model outcomes are strongly influenced by zooplankton feeding, suggesting that ecosystem dynamics may be sensitive to

changes in prey-size selection at the community level.

Zooplankton prey selectivity may be altered at the community level through taxonomic shifts. Copepods can make up 80% of the total abundance of zooplankton in some locations, and small pelagic copepods (<1 mm) may be the most abundant metazoans on earth (Turner 2004). Thus, most trophic interactions in the plankton likely involve copepods, which tend to feed as specialists with relatively large predator–prey size ratios (Fuchs & Franks 2010). However, there is evidence that community dynamics are altered both by invasions of more generalist taxa such as cladocerans (Mines et al. 2013) and by invasions of gelatinous taxa that have smaller predator–prey size ratios than copepods, including some schyphomedusae and ctenophores (Deason & Smayda 1982, Purcell 1992, Schneider & Behrends 1998, Fuchs & Franks 2010). Jellyfish blooms or invasions may alter trophic dynamics at the community level by increasing the frequency at which feeding interactions are characterized by a small predator–prey size ratio.

The schyphomedusa *Chrysaora quinquecirrha* (sea nettle) has become more common in parts of Barnegat Bay–Little Egg Harbor Estuary in New Jersey, USA, and may cause trophic interactions to vary spatially. Human populations have increased most rapidly in the northern portions of the estuary and have enlarged the area of hardened substrates that enable *C. quinquecirrha* to reproduce asexually (Carter 1997, Lathrop & Bognar 2001, Wieben & Baker 2009, Bologna 2011). In the north, this increase in substrate availability, combined with salinities in the preferred range (Decker et al. 2007), has facilitated increases in summertime *C. quinquecirrha* abundance over the last 2 decades (Kennish 2007, Bologna 2011). Sea nettles have smaller average predator–prey size ratios than copepods (Fuchs & Franks 2010), and their blooms may alter community dynamics in the north. We used the limited geographic range of *C. quinquecirrha* to compare plankton community metrics among sites in the estuary with and without the influence of invading gelatinous zooplankton.

For this study, the Barnegat Bay–Little Egg Harbor Estuary (BBLEH) was divided into northern and southern regions with a dividing line just south of the Toms River mouth (Fig. 1). Compared to the southern region, the northern region has lower salinity (Fig. 1), more hardened substrates (Carter 1997, Lathrop & Bognar 2001), higher *C. quinquecirrha* abundance (Bologna 2011), more nutrient loading (Wieben &
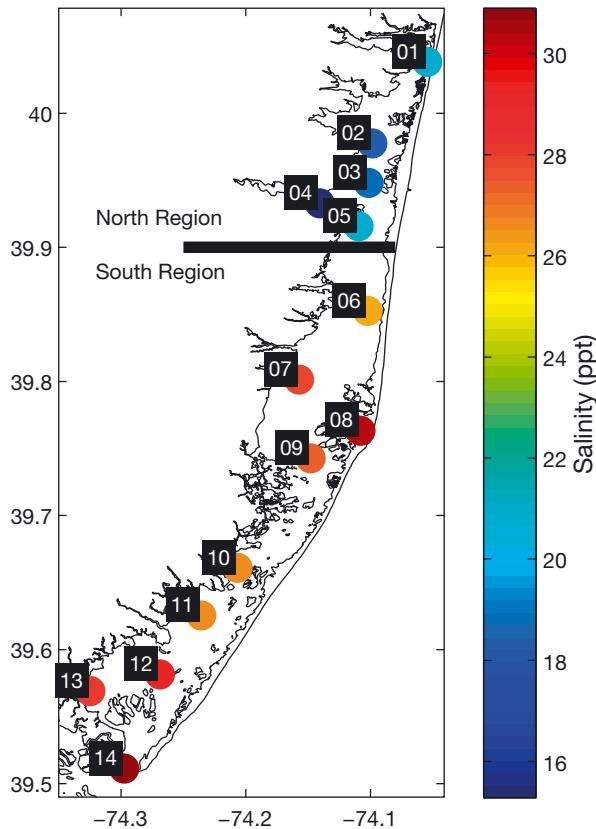
Fig. 1. Surface salinity in Barnegat Bay–Little Egg Harbor Estuary, New Jersey (USA), for July and August 2012. Sites are numbered, and the thick solid line denotes the division between northern and southern sites (data courtesy of New Jersey Department of Environmental Protection, publicly available at www.state.nj.us/dep/barnegatbay/bbmap viewer.htm)

Baker 2009), and larger phytoplankton (Olsen & Mahoney 2001). These differences in adjacent regions provide an opportunity to study the consequences of *C. quinquecirrha* presence or absence within a single system.

This study examined plankton community dynamics at various sites throughout BBLEH using a highly resolved NPZ model (Fuchs & Franks 2010). The model assumes that zooplankton predation can be described as a community average that will change if zooplankton taxonomic shifts occur. The objectives of the study were (1) to simulate copepod-like and jellyfish-like hypothetical plankton communities, (2) to compare model results to observational data from BBLEH, and (3) to test whether the presence of *C. quinquecirrha* altered plankton community dynamics. Data were available from 14 sites in the estuary, including 5 sites in the northern region and 9 sites in the southern region. We predicted that dynamics

would be more copepod-like in the southern region and more jellyfish-like the northern region, because *C. quinquecirrha* abundance is higher in the north.

## MATERIALS AND METHODS

### NPZ Model

We simulated hypothetical plankton communities using the Fuchs & Franks (2010) model of nutrients, phytoplankton, and zooplankton:

$$N(t) = N_T - \int P(x,t)\,dx - \int Z(x,t)\,dx \qquad (1)$$

$$\frac{\delta P(x,t)}{\delta t} = \qquad\qquad\qquad\qquad\qquad (2)$$
$$P(x,t)\left(-\lambda + \mu_{max}(x)\frac{N(t)}{N(t)+k_s} - g\int F^-(x,y)Z(y,t)\,dy\right)$$

$$\frac{\delta Z(x,t)}{\delta t} = Z(x,t)\left(-\delta - g\int F^-(x,y)Z(y,t)\,dy\right.$$
$$\left. + \gamma g\int F^+(y,x)[P(y,t)+Z(y,t)]\,dy\right) \qquad (3)$$

For this model, $N$ is free nutrients, $P$ is phytoplankton biomass, $Z$ is zooplankton biomass, $N_T$ is total nutrients, $x$ is organism size (equivalent spherical diameter on a $\log_{10}$ scale), $y$ is a dummy variable for integrating over size, $t$ is time, $\lambda$ is phytoplankton death rate, $\mu_{max}$ is maximum phytoplankton growth rate, $k_s$ is the half-saturation constant for nutrient uptake by phytoplankton, $g$ is zooplankton grazing rate, $\delta$ is zooplankton death rate, $\gamma$ is zooplankton assimilation efficiency, $F^-$ is the feeding kernel, and $F^+$ is the redistribution kernel (see Table 1 for a summary of symbols and their definitions). Total nutrients ($N_T$) are conserved, and phytoplankton and zooplankton biomass ($P$ and $Z$) are recycled to free nutrients ($N$) through mortality ($\lambda$ and $\delta$) and sloppy feeding ($1 - \gamma$). The kernels ($F^-$ and $F^+$) are community-averaged probability distributions that control size-dependent predation (biomass loss from prey and biomass gain to predators, respectively) along the size spectrum. The feeding kernel ($F^-$) is a Laplace distribution defined by the community-averaged mean $\log_{10}$ prey–predator size ratio ($-m$) and the standard deviation of the community-averaged $\log_{10}$ prey size distribution ($s$). The redistribution kernel ($F^+$) is a Laplace distribution defined by $m$ and $s$. All model parameters were held constant among simulations, except $N_T$, $m$, and $s$ (see 'Parameter selection' below).

Table 1. Definitions of symbols used in this study

| Symbol | Description | Value | Unit |
|---|---|---|---|
| $a$ | Allometric coefficient | 5 | $\mu m^b\,d^{-1}$ |
| $b$ | Allometric exponent | −0.75 | |
| $F^-$ | Feeding kernel | | |
| $F^+$ | Redistribution kernel | | |
| $g$ | Feeding rate | 7 | $\mu mol\,d^{-1}$ |
| $k_s$ | Half-saturation constant | 35 | $\mu mol$ |
| $m$ | Mean of $\log_{10}$ predator–prey size ratio | 0.638 to 2 | |
| $N$ | Free nitrogen | | $\mu mol\,l^{-1}$ |
| $N_T$ | Total nitrogen | 2.5 to 50 | $\mu mol\,l^{-1}$ |
| $P$ | Phytoplankton biomass | | $\mu mol\,l^{-1}$ |
| $s$ | Standard deviation of $\log_{10}$ prey size | 0.15 to 0.3 | $\log_{10}\,\mu m$ |
| $x$ | $\log_{10}$ of equivalent spherical diameter | | $\log_{10}\,\mu m$ |
| $Z$ | Zooplankton biomass | | $\mu mol\,l^{-1}$ |
| $\gamma$ | Assimilation efficiency | 0.7 | |
| $\delta$ | Zooplankton mortality | 0.17 | $d^{-1}$ |
| $\lambda$ | Phytoplankton mortality | 0.017 | $d^{-1}$ |
| $\mu_{max}$ | Maximum phytoplankton growth rate | $a10^{bx}$ | $d^{-1}$ |

Some numerical details were changed from the model version of Fuchs & Franks (2010) to provide greater flexibility in simulations. The time step was reduced to 0.2 d to ensure stability of high nutrient simulations ($N_T \geq 40$). The model was considered to be at quasi-equilibrium when the change in both $\Sigma P$ and $\Sigma Z$ between 2 consecutive time steps was less than $N_T \times 10^{-10}$. However, the quasi-equilibrium threshold was loosened by 1 to 4 orders of magnitude for 12 simulations that were slow to converge. Quasi-equilibrium values will be denoted with asterisks hereafter (e.g. $N^*$ is quasi-equilibrium free nutrient).

## Parameter selection: $N_T$, $m$, and $s$

Model simulations covered a range of nutrient conditions and zooplankton community types by varying $N_T$, $m$, and $s$. In all, 120 simulations were run using 20 $N_T$ values and 6 $m$–$s$ pairs (hereafter referred to as feeding regimes) in all possible combinations. Feeding regime and $N_T$ were held constant within each separate simulation.

Values of $N_T$ were selected to encompass nutrient conditions ranging from oligotrophic to eutrophic. The maximum $N_T$ value was set using observed total nitrogen values in BBLEH, which is highly eutrophic (Kennish et al. 2007). The highest mean total nitrogen concentration at any site in the estuary for July to August 2012 was 51.9 μmol N l$^{-1}$ (see the following section for observational data details). Model simulations used $N_T$ values ranging from 2.5 to 50 μmol N l$^{-1}$.

Feeding regimes were selected to encompass a broad range of zooplankton feeding preferences that may be present in BBLEH. One regime (Regime 1) was based on copepod feeding preferences, because copepods are numerically dominant in the estuary's mesozooplankton (Sandine 1984). Size-structured feeding data are lacking for the common copepod species in Barnegat Bay (i.e. *Acartia hudsonica*, *A. tonsa*, and *Oithona colcarva*; Sandine 1984), so the copepod-dominated regime was defined using the mean copepod feeding preference calculated by Fuchs & Franks (2010) ($m$ = 2, $s$ = 0.15). Another regime (Regime 5) was based on *Chrysaora quinquecirrha* feeding preferences, because *C. quinquecirrha* may be ecologically important zooplankton and are increasing in abundance in the estuary (Kennish 2007). *C. quinquecirrha* feeding preference ($m$ = 0.638, $s$ = 0.162; Cowan & Houde 1993, Purcell & Cowan 1995, Suchman & Sullivan 1998) is similar to another abundant jellyfish in the estuary (*Mnemiopsis leidyi*), so Regime 5 will be referred to as jellyfish-dominated. Three intermediate regimes (Regimes 2 to 4) were defined assuming a linear transition from copepod-dominated to jellyfish-dominated feeding parameters. The regimes defined to this point differ in $m$, but have similar $s$. We also included the generalist regime (Regime 6) from Fuchs & Franks (2010) for comparison purposes ($m$ = 1.2, $s$ = 0.3). The generalist regime has a higher $s$ than the other regimes, but an intermediate $m$.

## Available observational data

We compared model results to publicly available data from water-quality monitoring by the New Jersey Department of Environmental Protection (NJDEP; accessible at www.state.nj.us/dep/barnegatbay/bbmapviewer.htm). Data were collected at 14 sites in BBLEH from June 2011 to December 2012. Sampling frequency was ~1 to 4 samples mo$^{-1}$, except for an intense sampling effort in July and August 2012 when frequency was ~26 to 27 samples mo$^{-1}$. Unless otherwise noted, analyses were performed using July/August 2012 data, which coincided with the usual *C. quinquecirrha* bloom period (Decker et al. 2007). Measurements used here include surface and bottom total nitrogen (mg l$^{-1}$), sur-

face and bottom chlorophyll *a* (chl *a*, μg l$^{-1}$), surface dissolved nitrate plus nitrite (mg l$^{-1}$), surface dissolved ammonia (mg l$^{-1}$), and surface particulate organic carbon (mg l$^{-1}$). Zooplankton data from the same time period were collected at different sampling sites and frequencies, and the data were reported as abundances of identifiable taxa (P. Bologna & J. Gaynor unpubl. data). These data were unsuitable for comparison to modeled zooplankton biomass ($\Sigma Z^\star$), so we focused our analysis on nutrients and phytoplankton. Field-sampled total nitrogen, nitrate plus nitrite and ammonia, and chl *a* are comparable to the NPZ model input total nitrogen ($N_T$), output free nitrogen ($N^\star$), and phytoplankton biomass ($\Sigma P^\star$), respectively. For comparisons to model outputs, field-sampled variables were converted to units of nitrogen concentration (methods detailed below). Hereafter, NPZ model values will be referred to by the appropriate abbreviation (e.g. $N_T$), and observational data will be preceded by 'Barnegat' (e.g. Barnegat total nitrogen).

Barnegat total nitrogen was measured with EPA Method 351.4 (EPA 1979), which measures all nitrogen species except $N_2$ gas. The measurement includes nitrogen bound up in cells (H. Pang pers. comm.). Therefore, Barnegat total nitrogen is the sum of all biologically relevant nitrogen and is analogous to NPZ model input $N_T$. For comparison to $N_T$, Barnegat total nitrogen was converted from mg N l$^{-1}$ to μmol N l$^{-1}$.

Barnegat dissolved nitrate plus nitrate and dissolved ammonia were measured with EPA Method 353.4 (EPA 1997) and Standard Method 4500-NH3 (APHA 2011): G, respectively. Barnegat dissolved nitrate plus nitrite is reported in mg N l$^{-1}$, while Barnegat dissolved ammonia is reported in mg of ammonia l$^{-1}$. Barnegat dissolved ammonia was converted to mg N l$^{-1}$ and added to Barnegat nitrate plus nitrate to generate Barnegat dissolved inorganic nitrogen (excluding $N_2$ gas). Barnegat dissolved inorganic nitrogen represents free bio-available nitrogen and is analogous to NPZ model output $N^\star$. For comparison to $N^\star$, calculated Barnegat dissolved inorganic nitrogen was converted from mg N l$^{-1}$ to μmol N l$^{-1}$.

Barnegat chl *a* was measured with Standard Method 10200-H (APHA 2011), reported as mg chl *a* l$^{-1}$. For comparison to NPZ model units, measurements of chl *a* were converted to nitrogen concentration using cellular mass ratios for carbon to chl *a* (C:chl) and carbon to nitrogen (C:N). The C:chl and C:N were either calculated empirically from BBLEH field data or obtained from the literature, as detailed below. After the mass ratios were applied, Barnegat chl *a* was converted from mg N l$^{-1}$ to μmol N l$^{-1}$ for comparison to NPZ model output $\Sigma P^\star$.

Several values were used for the mass ratios, because these ratios can vary spatially and temporally based on the abiotic conditions and the taxonomic makeup of the phytoplankton community. An estuary-specific estimate of C:chl was derived from the available BBLEH data by performing a linear regression on particulate organic carbon and chl *a*, where the slope of this regression gives an estimate of C:chl (Strickland 1960, Banse 1977). The slope can be biased by covariation between phytoplankton, zooplankton, and detrital carbon (Menzel & Ryther 1964, Riley 1965, Banse 1977), and additional error is caused by intra-annual variability in C:chl (Cerco & Noel 2004). To limit these errors, we used Barnegat particulate organic carbon and chl *a* data from July and August 2011. No particulate organic carbon data were available for 2012. After removal of 1 outlier, the regression yielded a C:chl near 150 (Fig. 2). Nearby Chesapeake Bay has a C:chl of ~50 during July and August (Cerco & Noel 2004), but differs from BBLEH in size, morphology, and salinity range. Both C:chl
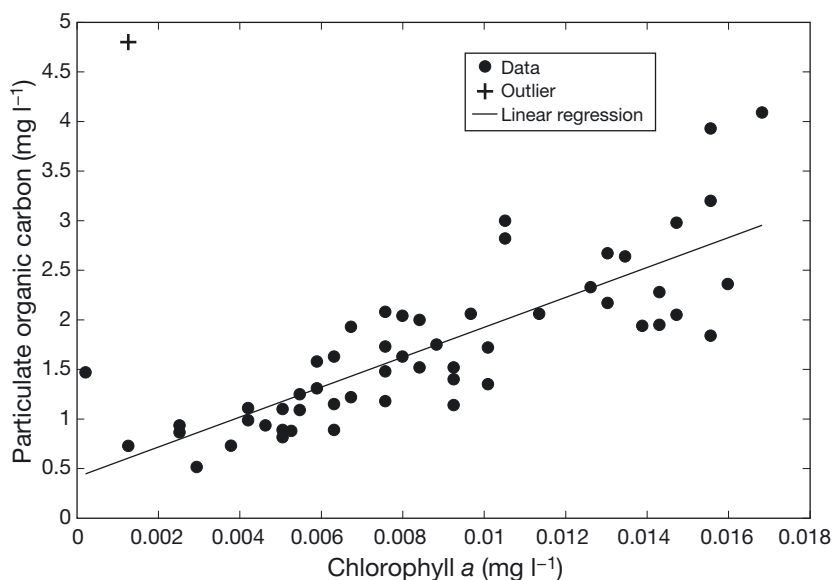


Fig. 2. Barnegat-derived C:chl ratio: regression of particulate organic carbon and chl *a* in Barnegat Bay–Little Egg Harbor Estuary from July and August 2011. The regression equation is $y = 150x + 0.42$ ($R^2 = 0.6586$). Trendline slope is the carbon to chl *a* ratio (mass:mass). One outlier (+) was excluded prior to linear regression (data source as in Fig. 1)

ratios were used in the analysis to encompass uncertainty associated with the value. However, the Barnegat C:chl is considered more appropriate, because it was derived in the estuary of interest.

Estimates of C:N could only be obtained from previous studies on plankton chemical composition. C:N ratios vary among taxa and range from 3.44 to 6.45 for dinoflagellates (Menden-Deuer & Lessard 2000), 4.5 to 8.8 for pico- and nanoplankton (Verity et al. 1992), and 3.5 to 25.4 for diatoms (Brzezinski 1985). To encompass the uncertainty associated with community-averaged C:N, 3 values were selected: low (3.5), high (12), and Redfield ratio (5.67; Redfield et al. 1963). All 3 C:N ratios were used in the analysis to encompass the uncertainty associated with the value. The Redfield C:N is considered most appropriate, because it is a community-averaged value.

## Processing of observational data

Several NPZ model variables were selected for comparison to Barnegat data. Model variables with comparable observational data include $N_T$, $N^*$, and $\sum P^*$ (see above). Ratios of these variables, $N^*/N_T$, $\sum P^*/N_T$, and $\sum P^*/N^*$ were also used for comparison. Ratios were calculated samplewise from the observational data, and if either value required was missing or 'below detection limit,' the ratio for that sample was excluded. However, calculated arithmetic means for Barnegat dissolved inorganic nitrogen were sensitive to how 'below detection limit' samples were treated (i.e. if samples were excluded, treated as 0, or treated as a value in between), because Barnegat dissolved nitrate plus nitrate values were typically close to the detection limit. Additionally, the data were asymmetrically distributed, so the arithmetic mean is a suboptimal estimate of central tendency. Concentration data with a low mean and high variance often have a lognormal distribution (Limpert et al. 2001), so we estimated summary statistics by fitting the data with lognormal curves and using a Monte Carlo procedure (Fig. 3). This approach is more appropriate than use of an arithmetic mean and reduces uncertainty from samples below the detection limit.

To ensure that a lognormal distribution was appropriate, we examined all samples collected in the estuary, assuming that they were drawn from the same
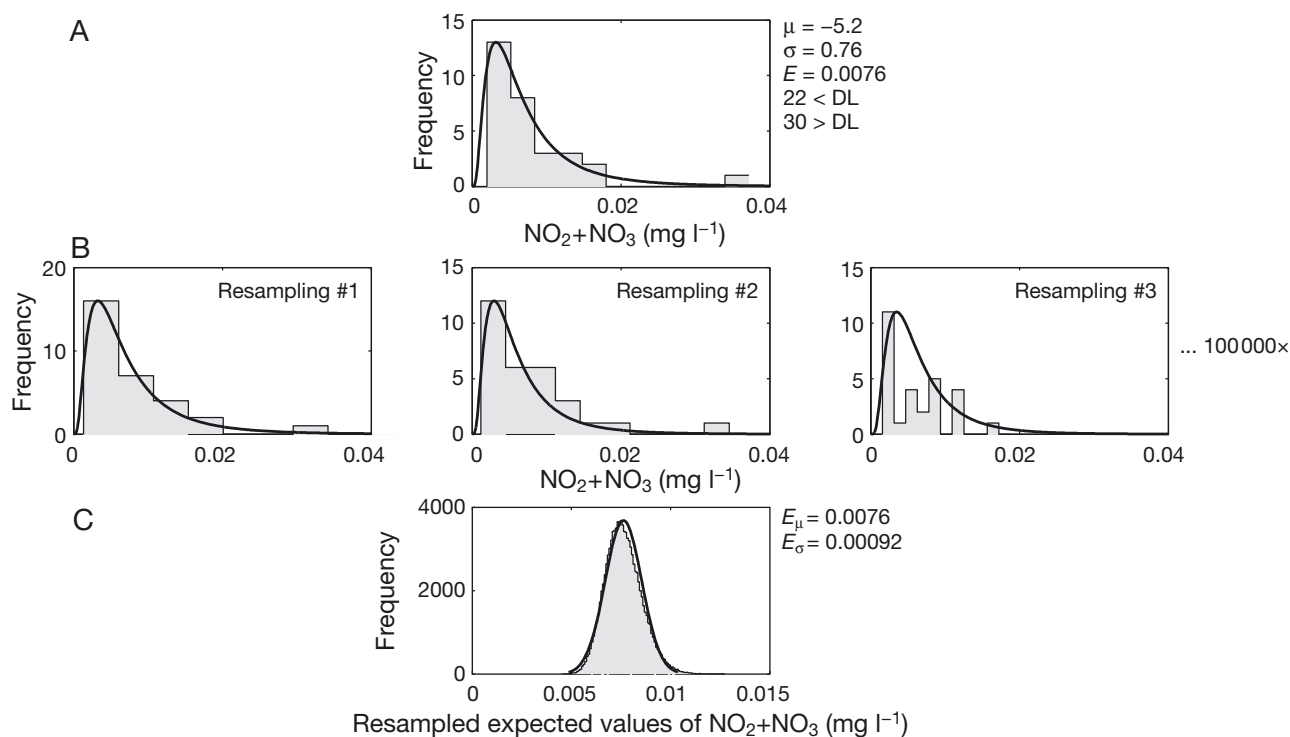


Fig. 3. Example of the Monte Carlo method, which was used to generate 95% confidence intervals and reduce the uncertainty due to the detection limit. For simplicity, this example uses dissolved nitrate plus nitrite data instead of dissolved inorganic nitrogen, which requires fitting and resampling for both dissolved nitrate plus nitrite and dissolved ammonia. (A) Histogram and lognormal fit for the data. Fit parameters ($\mu$ and $\sigma$), expected value of the fit ($E$), and the number of samples below and above detection limit (<DL and >DL) are reported. (B) Examples of resampled data fitted to a new lognormal distribution (solid line). Resampling was repeated 100 000 times and expected values were recorded. (C) Resampled expected values fitted to a normal distribution. The mean ($E_\mu$) and standard deviation ($E_\sigma$) of the normal fit are reported

distribution class. There were too few samples to reliably determine a distribution class for individual sites. Histograms of all measurement variables were non-normal (skewed right), and Lilliefors tests confirmed that most measurement data could be treated as lognormal. Barnegat dissolved inorganic nitrogen (i.e. the sum of Barnegat dissolved nitrate plus nitrate and Barnegat dissolved ammonia) also appeared to be lognormally distributed. The derived ratios (e.g. $\sum P^*/N^*$) should also be lognormally distributed because lognormal distributions are self-replicating by division.

We used curve fitting and Monte Carlo simulations to estimate expected values and 95% confidence intervals. To calculate the expected values, a lognormal distribution was fitted to each measurement variable at each site, excluding all samples that were below detection limit. The mean of the lognormal distribution ($e^{\mu+\sigma^2/2}$, where $\mu$ and $\sigma$ are the mean and SD of the natural logarithm of the data) was considered the expected value. We then randomly re-sampled the fitted lognormal distributions for the same number of samples as in the original data set, fit a new lognormal distribution to the re-sampled data, and calculated a re-sampled mean. This re-sampling procedure was repeated 100 000 times. The re-sampled means were normally distributed, and their spread represented the uncertainty associated with the given sample size. The 95% confidence interval is given by 1.96 SDs above and below the average of the re-sampled means. For ratios calculated from multiple measured values (i.e. $N^*$, $N^*/N_T$, $\sum P^*/N_T$, and $\sum P^*/N^*$), re-sampled data were generated from each measurement distribution, then added/divided appropriately and fitted to a new lognormal distribution. The estimated expected values for observational Barnegat data were used for model-to-data comparisons.

### Model-to-data comparisons

We quantified the degree of similarity between model outputs and Barnegat data using sums of squared error. The Barnegat-derived C:chl ratio and Redfield C:N ratio were used for all applicable calculations. Model outputs for $N^*$, $N^*/N_T$, $\sum P^*$, $\sum P^*/N_T$, and $\sum P^*/N^*$ were plotted against $N_T$ and $N^*$ with site observational data overlaid. Often site $N_T$ values did not match those simulated in the model, so model outputs were interpolated to the appropriate $N_T$. Data from each site were compared to interpolated model outputs for each of the 6 feeding regimes.

The overall differences between the northern and southern region of BBLEH were also examined. Analysis was similar to the site comparisons mentioned above, but we then summed the squared error for all sites within each region. The feeding regime with the smallest sum of squared error was considered best for describing that region. This calculation was performed for $N^*$, $N^*/N_T$, $\sum P^*$, $\sum P^*/N_T$, and $\sum P^*/N^*$. This analysis was repeated using all C:chl and C:N ratios to assess whether the uncertainty in these ratios could affect the comparisons.

### RESULTS

In general, NPZ model outputs clustered into 3 groups: Regimes 1 and 2, Regimes 3 and 4, and Regimes 5 and 6, which we refer to hereafter as copepod-dominated, intermediate, and jellyfish-dominated, respectively. At a given level of total nutrients, copepod regimes typically had the highest phytoplankton biomass (i.e. $\sum P^*$, $\sum P^*/N_T$, $\sum P^*/N^*$), whereas jellyfish regimes had the highest free nutrients (i.e. $N^*$ and $N^*/N_T$).

### Site comparisons (Barnegat C:chl and Redfield C:N only)

There was a clear separation in total nitrogen and phytoplankton biomass between sites in the northern and southern regions of BBLEH. All northern sites had greater total nitrogen and phytoplankton biomass than any southern site (Fig. 4A,B). Although data were variable, most sites were most similar to the copepod-dominated model outputs for both the $\sum P^*$ vs. $N_T$ and $\sum P^*$ vs. $N^*$ plots. The exceptions were Sites 2, 4, 9, 10, and 13 for $\sum P^*$ vs. $N_T$ and Sites 4, 9, and 11 for $\sum P^*$ vs. $N^*$. Sites 2, 10, and 13 for $\sum P^*$ vs. $N_T$ and Site 11 for $\sum P^*$ vs. $N^*$ were more similar to the intermediate model outputs. Site 9 was more similar to the jellyfish-dominated model outputs. Site 4 was dissimilar to all model outputs (Fig. 4A,B).

With a few exceptions, northern and southern sites had relatively similar ratios of free nitrogen to total nitrogen and phytoplankton biomass to free nitrogen. In general, the northern sites tended to have lower free nitrogen to total nitrogen ratios than the southern sites (Fig. 5). However, this was not true for Site 4 (a northern site with a high $N^*/N_T$) and Sites 6 and 7 (southern sites with a low $N^*/N_T$; Fig. 5). Conversely, the northern sites tended to have higher phytoplankton biomass to free nitrogen ratios than
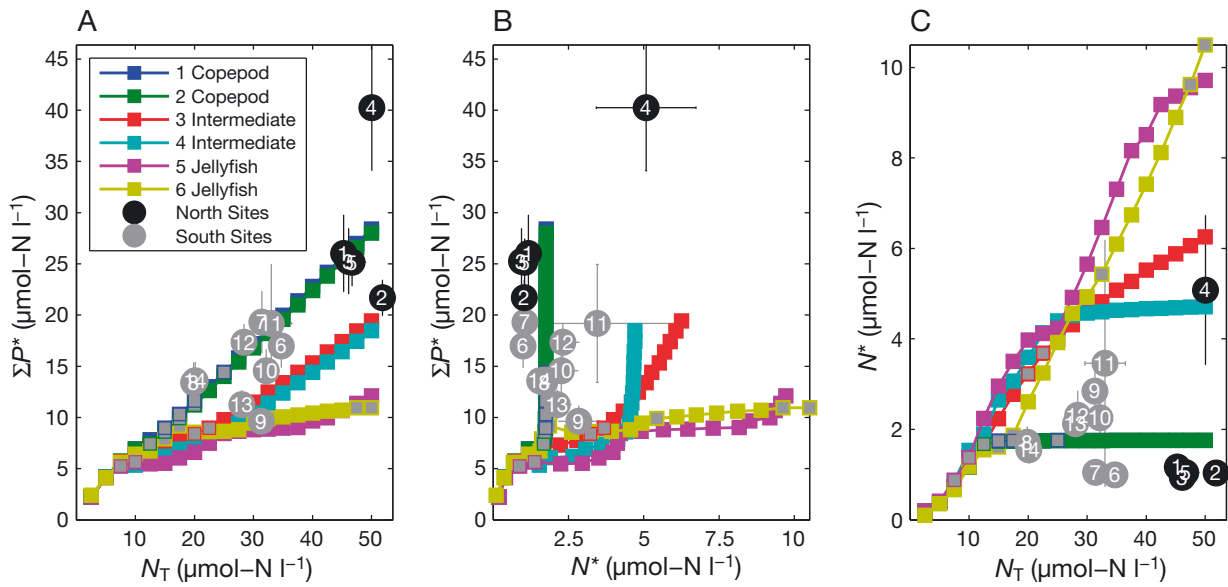
Fig. 4. Model-to-data comparison of phytoplankton biomass and free nitrogen. Barnegat Bay–Little Egg Harbor Estuary observational data for July and August 2012 are overlaid on nutrient–phytoplankton–zooplankton (NPZ in subsequent figure legends) model outputs. (A) Phytoplankton biomass ($\Sigma P^\bullet$) vs. total nitrogen ($N_T$). (B) Phytoplankton biomass ($\Sigma P^\bullet$) vs. free nitrogen ($N^\bullet$). (C) Free nitrogen ($N^\bullet$) vs. total nitrogen ($N_T$). Circles with error bars are expected values and 95 % confidence intervals for data at sites denoted by numbers. Circle color denotes region (black: north, gray: south). Colored lines denote 50 model feeding parameterizations (Regimes 1 and 2 are copepod-dominated, Regimes 3 and 4 are intermediate, and Regimes 5 and 6 are jellyfish-dominated). Squares with gray fills denote model simulations that required loosened quasi-equilibrium thresholds (data source for circles as in Fig. 1)



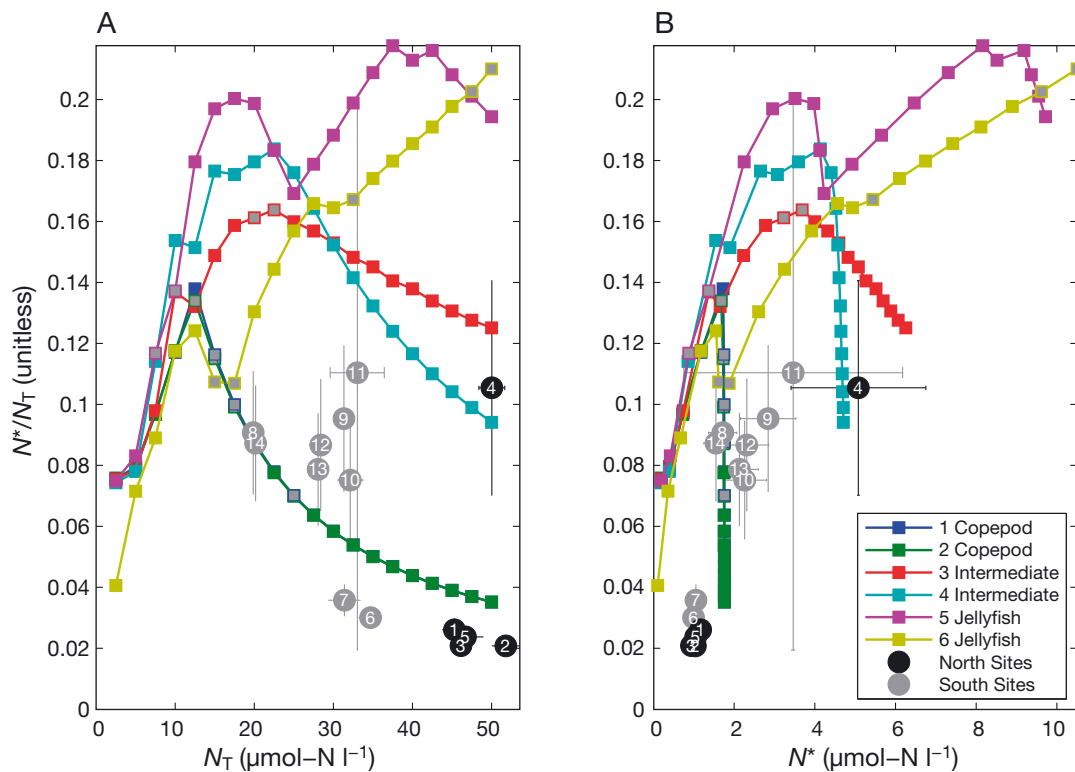Fig. 5. Model-to-data comparison of free nitrogen to total nitrogen ratio. Barnegat Bay–Little Egg Harbor Estuary observational data for July and August 2012 are overlaid on NPZ model outputs. (A) Free nitrogen to total nitrogen ratio ($N^\bullet/N_T$) vs. total nitrogen ($N_T$). (B) Free nitrogen to total nitrogen ratio ($N^\bullet/N_T$) vs. free nitrogen ($N^\bullet$). Symbols, lines, and data source as in Fig. 4
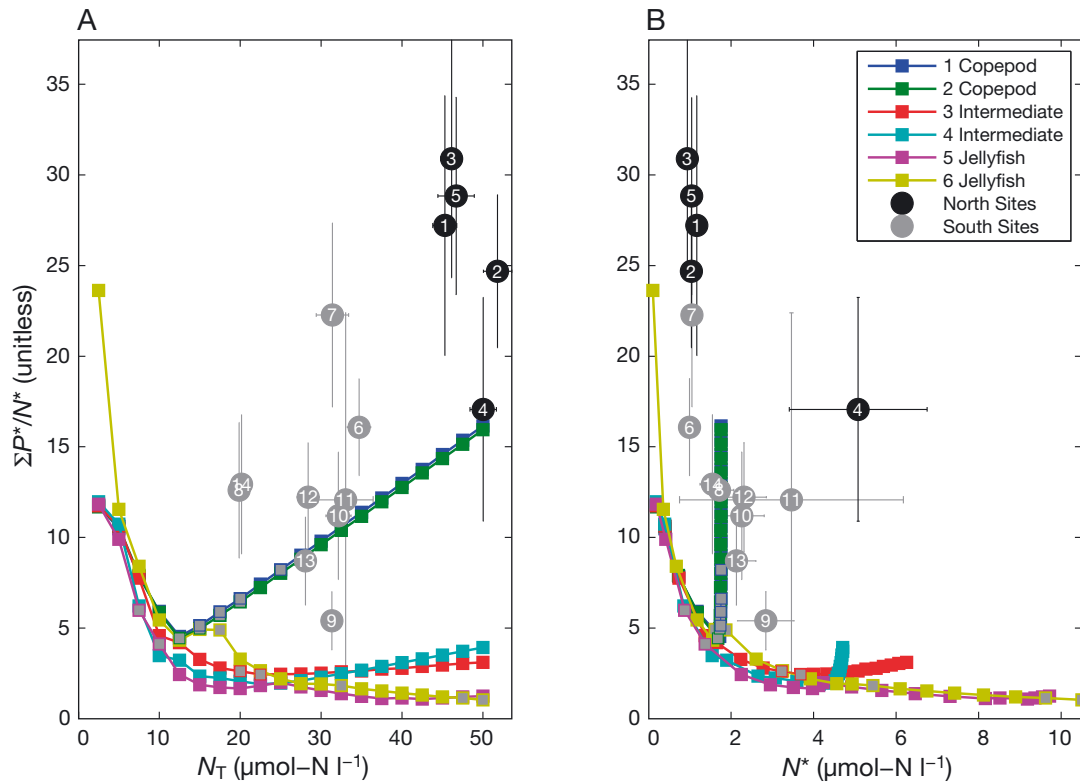
Fig. 6. Model-to-data comparison of phytoplankton biomass to free nitrogen ratio. Barnegat Bay–Little Egg Harbor Estuary observational data for July and August 2012 are overlaid on NPZ model outputs. (A) Phytoplankton biomass to free nitrogen ratio ($\Sigma P^*/N^*$) vs. total nitrogen ($N_T$). (B) Phytoplankton biomass to free nitrogen ratio ($\Sigma P^*/N^*$) vs. free nitrogen ($N^*$). Symbols, lines, and data source as in Fig. 4

southern sites (Fig. 6). The notable exceptions to this pattern were Sites 4 (a northern site with lower $\Sigma P^*/N^*$) and 7 (a southern site with higher $\Sigma P^*/N^*$). For all related plots ($N^*/N_T$ vs. $N_T$, $N^*/N_T$ vs. $N^*$, $\Sigma P^*/N^*$ vs. $N_T$, and $\Sigma P^*/N^*$ vs. $N^*$), most sites in the north and south were similar to the copepod-dominated model outputs (Figs. 5 & 6). The only exceptions were Sites 4 and 11 for both $N^*/N_T$ plots and Site 9 for both $\Sigma P^*/N^*$ plots. Sites 4 and 11 for $N^*/N_T$ and Site 9 for $\Sigma P^*/N^*$ were more similar to the intermediate model outputs. Despite being most similar to the copepod-dominated model outputs, Sites 1 to 5 and 7 were poorly matched by any regime for both $\Sigma P^*/N^*$ plots (Figs. 5 & 6). The large 95% confidence intervals for free nitrogen to total nitrogen ratio and phytoplankton biomass to free nitrogen ratio are caused by a low sample size for the measurements that make up free nitrogen. Dissolved nitrate plus nitrite had the greatest percentage of samples below detection limit, followed by dissolved ammonia (data not shown).

We found no clear north to south gradient in the other parameters analyzed. Free nitrogen was similar for all sites except Sites 4 and 11 (Fig. 4C). The phytoplankton biomass to total nitrogen ratios at many of

the northern sites fall in the middle of the range observed for southern sites (Fig. 7). For both variables, the spread in values is greater for southern sites than northern sites. Free nitrogen values for northern sites are clustered near the bottom of the range of southern sites, except Site 4 (Fig. 4C). The phytoplankton biomass to total nitrogen ratios for northern sites are clustered in the center of the range for southern sites, except Site 4 (Fig. 7). Most sites in the north and south were most similar to the copepod-dominated model outputs for both $N^*$ vs. $N_T$ and $\Sigma P^*/N_T$ vs. $N_T$ plots (Figs. 4C & 7). The only exceptions were Sites 4 and 11 for $N^*$ vs. $N_T$ and Sites 2, 9, and 13 for $\Sigma P^*/N_T$ vs. $N_T$. Sites 4 and 11 for $N^*$ vs. $N_T$ and Sites 2 and 13 for $\Sigma P^*/N_T$ vs. $N_T$ were more similar to the intermediate model outputs. Site 9 for $\Sigma P^*/N_T$ vs. $N_T$ was more similar to the jellyfish-dominated model outputs. There was insufficient separation between copepod- and jellyfish-dominated model outputs in the $\Sigma P^*/N_T$ vs. $N^*$ to determine differences among BBLEH sites, although Site 4 was dissimilar to all model outputs (Fig. 7B).

Several sites consistently broke from the typical pattern of copepod-dominance in BBLEH. The sites that were most often similar to intermediate or jelly-
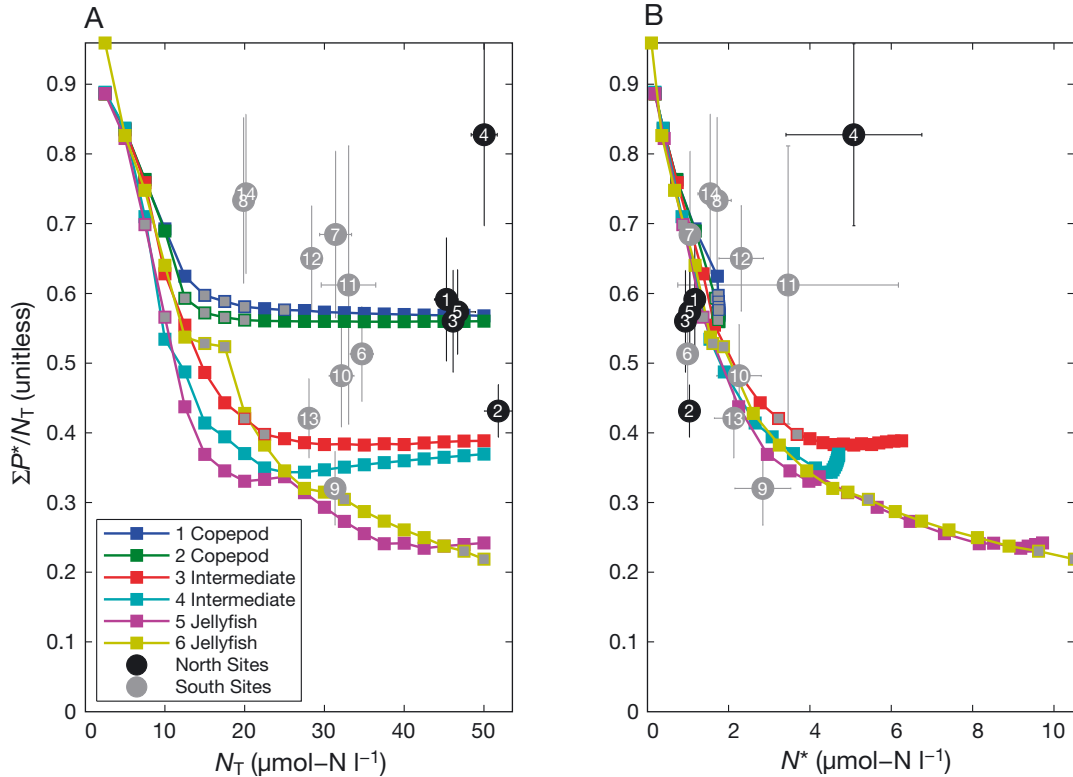
Fig. 7. Model-to-data comparison of phytoplankton biomass to total nitrogen ratio. Barnegat Bay–Little Egg Harbor Estuary observational data for July and August 2012 are overlaid on NPZ model outputs. (A) Phytoplankton biomass to total nitrogen ratio ($\Sigma P^\bullet/N_T$) vs. total nitrogen ($N_T$). (B) Phytoplankton biomass to total nitrogen ratio ($\Sigma P^\bullet/N_T$) vs. free nitrogen ($N^\bullet$). Symbols, lines, and data source as in Fig. 4

fish-dominated model outputs were Sites 4, 9, 11, and 13. However, Sites 4 and 11 may be unrepresentative of typical BBLEH summertime plankton communities. Site 4 is located at the Toms River mouth and was dissimilar from other northern sites for all observational data. Sampling at Site 11 was halted midway through the summer, so the dataset there is incomplete. Sites 8 and 14 had similar observational data with lower total nitrogen than the other southern sites. These sites are both located at ocean inlets and may differ from typical BBLEH summertime plankton communities.

was best described by feeding Regime 1 (Table 2). The southern region was similar, except that phytoplankton biomass was best described by feeding Regime 2 (Table 2).

Table 2. Best matching models for regional comparisons. The model feeding regimes that are most similar to observational site data are reported for various metrics and conversion ratios. Regimes 1 and 2 are copepod-dominated, Regimes 3 and 4 are intermediate, and Regimes 5 and 6 are jellyfish-dominated. Metrics listed are free nitrogen ($N^\bullet$), phytoplankton biomass ($\Sigma P^\bullet$), free nitrogen to total nitrogen ratio ($N^\bullet/N_T$), phytoplankton biomass to total nitrogen ratio ($\Sigma P^\bullet/N_T$), and phytoplankton biomass to free nitrogen ratio ($\Sigma P^\bullet/N^\bullet$). All combinations of the C:chl ratio (Barnegat-derived = 150, Chesapeake-derived = 50) and the C:N ratio (Redfield [RF] = 5.67, low [L] = 3.5, high [H] = 12) are shown. The most similar feeding regimes were determined by the lowest sum of squared error between the site observational data and the model output for the $N_T$ values observed at those sites. $N^\bullet$ and $N^\bullet/N_T$ are only reported once because those values are invariant to the mass ratio assumptions

| Metric | Region: | North | | | | | | South | | | | | |
|---|---|---|---|---|---|---|---|---|---|---|---|---|---|
| | C:chl: | Barnegat | | | Chesapeake | | | Barnegat | | | Chesapeake | | |
| | C:N: | RF | L | H | RF | L | H | RF | L | H | RF | L | H |
| $N^\bullet$ | | 1 | – | – | – | – | – | 1 | – | – | – | – | – |
| $\Sigma P^\bullet$ | | 1 | 1 | 5 | 6 | 4 | 6 | 2 | 1 | 5 | 5 | 5 | 5 |
| $N^\bullet/N_T$ | | 1 | – | – | – | – | – | 1 | – | – | – | – | – |
| $\Sigma P^\bullet/N_T$ | | 1 | 1 | 5 | 6 | 4 | 6 | 1 | 1 | 5 | 5 | 6 | 5 |
| $\Sigma P^\bullet/N^\bullet$ | | 1 | 1 | 2 | 4 | 2 | 4 | 1 | 1 | 3 | 3 | 2 | 4 |

## Regional comparisons (all C:chl and C:N)

Similar to site-specific comparisons, regional data most resembled the copepod-dominated model results when Barnegat C:chl and Redfield C:N were used. As a region, the north
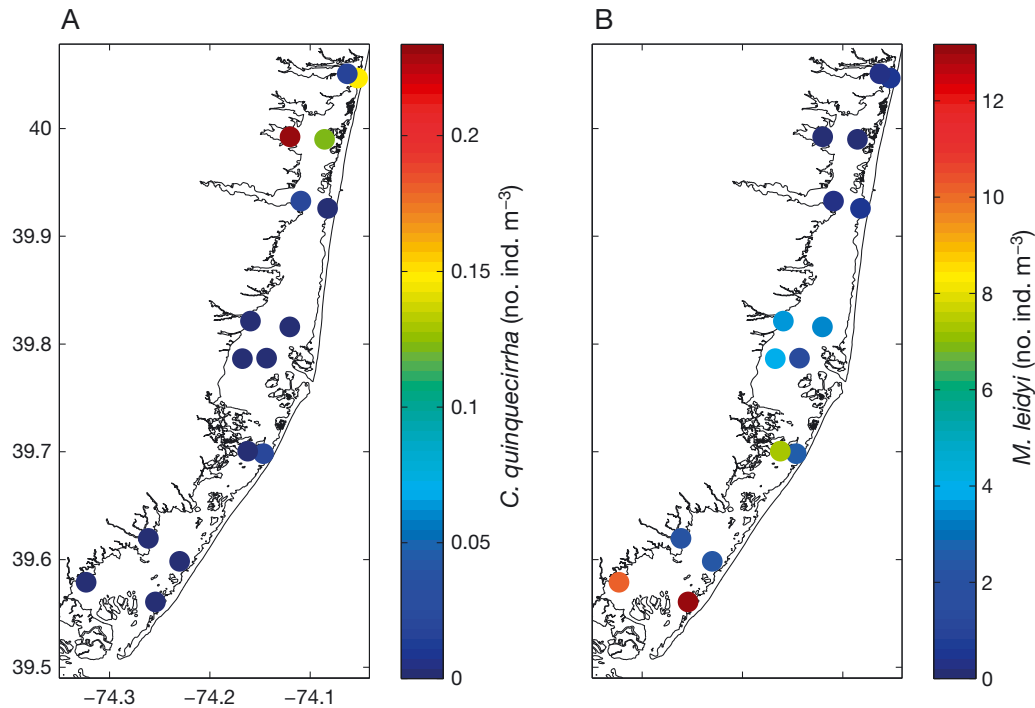
Fig. 8. Jellyfish densities at various sites in Barnegat Bay–Little Egg Harbor Estuary for July and August 2012. Panels show lift-net data for (A) *Chrysaora quinquecirrha* and (B) *Mnemiopsis leidyi* (P. Bologna & J. Gaynor unpubl. data)

Phytoplankton biomass, phytoplankton biomass to total nitrogen ratio, and phytoplankton biomass to free nitrogen ratio varied greatly depending on the C:chl and C:N ratio used. Depending on mass ratios used, the best feeding regime for phytoplankton biomass varied from 1 to 6 for northern sites and 1 to 5 for southern sites (Table 2). The best feeding regime for the phytoplankton biomass to total nitrogen ratio varied from 1 to 6 for both northern and southern sites (Table 2). The best feeding regime for the phytoplankton biomass to free nitrogen ratio varied from 1 to 4 in both northern and southern sites (Table 2).

Overall, the variability associated with using different combinations of mass ratios was greater than the variability between the northern and southern sites. For a given mass ratio, the feeding regimes that best described the north and south were similar for most variables examined. The north and south were more often best described by the same feeding regime than by different feeding regimes (Table 2). Even when the best feeding regime differed, both locations were often still best described by the same grouping (e.g. Regimes 1 and 2 are both copepod-dominated). When the grouping differed, the south was closer to jellyfish-dominance than the north (Table 2).

## DISCUSSION

### Barnegat Bay trophic interactions

Our results show an unexpected spatial pattern of plankton communities in BBLEH. We expected the jellyfish-dominated model output to be more similar to BBLEH plankton communities with higher *Chrysaora quinquecirrha* abundance (i.e. sites in the northern region). This study suggests the opposite, however; the most jellyfish-like site in the estuary was located in the southern region, where high salinity prevents *C. quinquecirrha* survival. The northern region, where *C. quinquecirrha* bloom, was modeled most accurately using a copepod-dominated feeding preference. Our results showed no evidence that increasing *C. quinquecirrha* abundances lead to more jellyfish-dominated community dynamics in BBLEH.

This seemingly counterintuitive result could be related to the distribution of other gelatinous taxa in BBLEH, specifically *Mnemiopsis leidyi*. Lift-net data from 2012 show that *M. leidyi* was the dominant gelatinous taxon, whose abundance was inversely related to *C. quinquecirrha* abundance in BBLEH during the summer (P. Bologna & J. Gaynor unpubl. data; Fig. 8). Tow data from the same surveys show similar results. *M. leidyi* is a ravenous grazer of

microzooplankton (Mountford 1980, Sandine 1984) and has similar feeding preferences to *C. quinquecirrha*. Higher abundances of *M. leidyi* in the south may partially explain why the southern region appeared to be more jellyfish-dominated than the northern region.

Predation by *C. quinquecirrha* could explain the spatial distribution of *M. leidyi*. Laboratory-measured clearance rates suggest that *C. quinquecirrha* can eliminate *M. leidyi* from Chesapeake Bay tributaries (Purcell & Cowan 1995). *M. leidyi* was absent from the northern region of BBLEH during summer 2012 (P. Bologna & J. Gaynor unpubl. data; Fig. 8B), even though *M. leidyi* has wide environmental tolerances (Purcell et al. 2001) and was unlikely to be excluded by physical/chemical factors. We suspect that *C. quinquecirrha* excluded *M. leidyi* from that region through predation.

Interactions between *C. quinquecirrha* and *M. leidyi* could reinforce the differences between the plankton communities in the north and south of BBLEH. By consuming *M. leidyi*, a voracious copepod predator, *C. quinquecirrha* may have indirectly caused the northern region of BBLEH to become more copepod-like. This idea is supported by evidence from Chesapeake Bay, where *M. leidyi* abundances fell and copepod standing stock rose when *C. quinquecirrha* became abundant (Feigenbaum & Kelly 1984). In addition, predation rates on shared prey (e.g. copepods) are lower when *C. quinquecirrha* and *M. leidyi* co-occur (Cowan & Houde 1992, Purcell et al. 1994). Alterations to the base of the food web, driven by *C. quinquecirrha* and *M. leidyi* interactions, may also impact higher trophic levels in BBLEH.

The potential for *C. quinquecirrha* to alter New Jersey's fisheries merits further study, because both *C. quinquecirrha* and *M. leidyi* feed on fish larvae (Cowan & Houde 1992) and may impact fish populations. Predation rates on ichthyoplankton are higher for *C. quinquecirrha* than for *M. leidyi* (Cowan & Houde 1992). When both taxa are present, however, ichthyoplankton predation is lower than expected because of the handling time required for *C. quinquecirrha* to consume *M. leidyi* (Cowan & Houde 1992). In locations where these taxa co-occur, *C. quinquecirrha* could reduce ichthyoplankton mortality through its interactions with *M. leidyi* (Cowan & Houde 1992, 1993). *C. quinquecirrha* predation on *M. leidyi* may also increase the standing stock of copepod prey available for more commercially important estuarine species (Feigenbaum & Kelly 1984). The direct effect of *C. quinquecirrha* on ichthyoplankton

and copepods would likely be negative for fisheries, while the indirect effects of reducing *M. leidyi* would likely be positive for fisheries. The net effect of *C. quinquecirrha* on New Jersey's fisheries would be influenced by the relative abundance of each jellyfish and is largely unknown.

Our results indicate that the impacts of a jellyfish invasion on community dynamics may vary depending on the taxa of invaders and presence of other gelatinous species. The outcome depends on the trophic level of the jellyfish and dynamics within the local ecosystem. An increase in *M. leidyi* abundance within BBLEH would likely cause the community-averaged feeding of the estuary to become more jellyfish-dominated, which appears to be true of the southern region of BBLEH (P. Bologna & J. Gaynor unpubl. data; Fig. 8). Additionally, the effect of *C. quinquecirrha* may have been different in the absence of *M. leidyi*. The presence of *M. leidyi* reduces *C. quinquecirrha* grazing rate on ichthyoplankton (Cowan & Houde 1992), while the presence of *C. quinquecirrha* influences the impact of *M. leidyi* on copepod standing stock (Feigenbaum & Kelly 1984). We originally predicted that abundant *C. quinquecirrha* would lead to jellyfish-dominated ecosystem dynamics, and this prediction may have been borne out in the absence of *M. leidyi*.

### Study limitations

The size-structured model uses an aggregated zooplankton type with limited utility for describing competition among jellyfish that have similar feeding preferences. Our primary focus was on sea nettles, which have received considerable attention as a nuisance invader. Given the different feeding preferences of jellyfish and copepods, our model initially seemed reasonable for testing effects of these groups on community dynamics in different regions of the estuary. However, the results identify weaknesses in our initial conceptual model of the system by demonstrating that top-down control is strongly influenced by competition within functional groups. The dynamics of this system may be better captured with a different model type.

The model used here may be better suited for studying the impacts of generalist invaders on a predominantly specialist system. The BBLEH system is dominated by jellyfish or copepods that differ mainly in their mean predator–prey size ratios (Fuchs & Franks 2010), but other systems have more distinct specialist–generalist interactions. At higher lati-

tudes, salp–krill oscillations dominate the zooplankton (Loeb et al. 1997, Atkinson et al. 2004) and can influence vertebrate predator populations (Reid & Croxall 2001) and chl *a* concentrations (Loeb et al. 1997). Krill have more generalist feeding preferences than any of the taxa in the present study, and salps have greater predator–prey size ratios and diet breadth (i.e. are more generalist) than krill (Fuchs & Franks 2010). In our study, the most generalist simulations (Regime 6) closely resembled those dominated by jellyfish. Based on these results, we expect that high-latitude, krill- or salp-dominated plankton communities may have higher free nutrient concentrations and lower phytoplankton biomass than those of lower-latitude, copepod-dominated communities with similar total nutrients. Krill–salp interactions may also have complex influences on trophic structure similar to those of *C. quinquecirrha* and *M. leidyi* in this study. Additional simulations would be required to explore these possibilities.

Some of the data used in this study were limited in usefulness because concentrations were often below the sensitivity of measurement methods used. Dissolved nitrate plus nitrite and dissolved ammonia had the highest incidence of samples 'below detection limit.' At all sites, 30 to 67 % of dissolved nitrate plus nitrite samples had to be excluded. These low nitrate plus nitrite concentrations are consistent with low nitrate and nitrate concentrations measured elsewhere at warm water temperatures (Kamykowski & Zentara 1986). Although we accounted for the excluded samples using a Monte Carlo approach, sample exclusion still may have reduced the accuracy of calculations by reducing the sample size that could be used for curve fitting. Concentrations were low, and uncertainty could cause a large error relative to the true concentration, particularly for any results involving $N^*$. These issues highlight the need for more sensitive measurements when sampling dissolved nitrate plus nitrite and dissolved ammonia in estuarine environments.

The results of this study were also greatly affected by the selection of the mass ratios (C:chl and C:N). Our interpretations are based on results using Barnegat C:chl and Redfield C:N. We consider those mass ratios to be the most appropriate, because C:chl was derived from Barnegat data for the appropriate time of year and no cellular nutrient concentration data were available to better constrain C:N. However, these ratios are highly variable among taxa (Brzezinski 1985, Verity et al. 1992, Menden-Deuer & Lessard 2000), as well as within taxa under various circumstances (Laws & Bannister 1980, Falkowski et

al. 1985). In cultured phytoplankton, C:chl ratios have been recorded from <20 to 500 (Laws & Bannister 1980, Falkowski et al. 1985). The wide ranges of these values makes it necessary to better constrain mass ratios for interpreting ecosystem data and comparing them to model outputs.

By using different C:chl and C:N ratios, the northern and southern regions of BBLEH could best fit either copepod-dominated or jellyfish-dominated ecosystems. Although the south was relatively more jellyfish-dominated regardless of the mass ratio used, it is undetermined whether the regions are overall jellyfish- or copepod-dominated. With more detailed and accurate C:chl and C:N data, it would have been possible to derive different ratios for the northern and southern regions of BBLEH. The northern region has larger phytoplankton cells and higher nutrient loading (Olsen & Mahoney 2001), both of which could cause variability in the C:chl and C:N ratios. Addressing the uncertainty in these ratios would require a multi-year study to assess the relative abundances and cellular stoichiometry of BBLEH taxa. Such data would enable a more nuanced analysis of plankton community dynamics.

Despite uncertainties in mass ratios and the limitations of the observational data, the results of this study demonstrate that *C. quinquecirrha* is involved in complex trophic interactions that impact ecosystem dynamics. In BBLEH, the presence of *C. quinquecirrha* apparently drives plankton communities to a more copepod-dominated state by eliminating planktivorous ctenophores.

LITERATURE CITED

Anderson TR, Gentleman WC, Sinha B (2010) Influence of grazing formulations on the emergent properties of a complex ecosystem model in a global ocean general circulation model. Prog Oceanogr 87:201–213

APHA (American Public Health Association) (2011) Standard methods for the examination of water and wastewater. American Public Health Association, Washington, DC

Atkinson A, Siegel V, Pakhomov E, Rothery P (2004) Long-term decline in krill stock and increase in salps within the Southern Ocean. Nature 432:100–103

Banas NS (2011) Adding complex trophic interactions to a

size-spectral plankton model: emergent diversity patterns and limits on predictability. Ecol Model 222: 2663–2675

Banse K (1977) Determining the carbon-to-chlorophyll ratio of natural phytoplankton. Mar Biol 41:199–212

Barnes C, Maxwell D, Reuman DC, Jennings S (2010) Global patterns in predator–prey size relationships reveal size dependency of trophic transfer efficiency. Ecology 91:222–232

Bogdan KG, Gilbert JJ (1982) Seasonal patterns of feeding by natural populations of *Keratella, Polyarthra*, and *Bosmina*: clearance rates, selectivities, and contributions to community grazing. Limnol Oceanogr 27:918–934

Bologna P (2011) Sea nettle (*Chrysaora quinquecirrha*) polyps in Barnegat Bay, NJ: a pilot assessment. Final Report to the Barnegat Bay Partnership. Available at http://bbp.ocean.edu/Reports/Assessment%20of%20sea %20nettle%20final%20project%20report.pdf

Brzezinski MA (1985) The Si:C:N ratio of marine diatoms: interspecific variability and the effect of some environmental variables. J Phycol 21:347–357

Carter GP (1997) Eight characterizing trends in the Barnegat Bay Watershed, Ocean County, New Jersey. Proceedings of The Barnegat Bay Ecosystem Workshop. Rutgers Cooperative Extension of Ocean County, Toms River, NJ. Available at www.state.nj.us/dep/dsr/barn.pdf

Cerco CF, Noel MR (2004) Process-based primary production modeling in Chesapeake Bay. Mar Ecol Prog Ser 282:45–58

Cowan JH Jr, Houde ED (1992) Size-dependent predation on marine fish larvae by ctenophores, scyphomedusae, and planktivorous fish. Fish Oceanogr 1:113–126

Cowan JH Jr, Houde ED (1993) Relative predation potentials of scyphomedusae, ctenophores and planktivorous fish on ichthyoplankton in Chesapeake Bay. Mar Ecol Prog Ser 95:55–65

Deason EE, Smayda TJ (1982) Ctenophore–zooplankton–phytoplankton interactions in Narragansett Bay, Rhode Island, USA, during 1972–1977. J Plankton Res 4: 203–217

Decker MB, Brown CW, Hood RR, Purcell JE and others (2007) Predicting the distribution of the scyphomedusa *Chrysaora quinquecirrha* in Chesapeake Bay. Mar Ecol Prog Ser 329:99–113

EPA (1979) Methods for chemical analysis of water and wastes. US Environmental Protection Agency, Washington, DC, EPA/600/4-79/020 (NTIS PB84128677)

EPA (1997) Methods for the determination of chemical substances in marine and estuarine environmental matrices. 2nd edn. EPA 600/R-97-072. www.epa.gov/nerlcwww/ordmeth.htm

Estes JA, Tinker MT, Williams TM, Doak DF (1998) Killer whale predation on sea otters linking oceanic and nearshore ecosystems. Science 282:473–476

Falkowski PG, Dubinsky Z, Wyman K (1985) Growth–irradiance relationships in phytoplankton. Limnol Oceanogr 30:311–321

Feigenbaum D, Kelly M (1984) Changes in the lower Chesapeake Bay food chain in presence of the sea nettle *Chrysaora quinquecirrha* (Scyphomedusa). Mar Ecol Prog Ser 19:39–47

Frank KT, Petrie B, Choi JS, Leggett WC (2005) Trophic cascades in a formerly cod-dominated ecosystem. Science 308:1621–1623

Fuchs HL, Franks PJS (2010) Plankton community proper-

ties determined by nutrients and size-selective feeding. Mar Ecol Prog Ser 413:1–15

González JM, Sherr EB, Sherr BF (1993) Differential feeding by marine flagellates on growing versus starving, and on motile versus nonmotile, bacterial prey. Mar Ecol Prog Ser 102:257–267

Hansen B, Bjørnsen PK, Hansen PJ (1994) The size ratio between planktonic predators and their prey. Limnol Oceanogr 39:395–403

Kamykowski D, Zentara S (1986) Predicting plant nutrient concentrations from temperature and sigma-*t* in the upper kilometer of the world ocean. Deep-Sea Res A Oceanogr Res Pap 33:89–105

Kennish MJ (2007) Barnegat Bay–Little Egg Harbor Estuary: ecosystem condition and recommendations. Technical Report. Rutgers University, Institute of Marine and Coastal Sciences, New Brunswick, NJ. Available at http: //jcnerr.org/research/PDFs/Barnegat%20Bay%20Indicators.pdf

Kennish MJ, Bricker SB, Dennison WC, Glibert PM and others (2007) Barnegat Bay–Little Egg Harbor Estuary: case study of a highly eutrophic coastal bay system. Ecol Appl 17:S3–S16

Lathrop RG Jr, Bognar JA (2001) Habitat loss and alteration in the Barnegat Bay region. J Coastal Res Spec Issue 32: 212–228

Laws EA, Bannister TT (1980) Nutrient- and light-limited growth of *Thalassiosira fluviatilis* in continuous culture, with implications for phytoplankton growth in the ocean. Limnol Oceanogr 25:457–473

Limpert E, Stahel WA, Abbt M (2001) Log-normal distributions across the sciences: keys and clues. Bioscience 51: 341–352

Loeb V, Siegel V, Holm-Hansen O, Hewitt R, Fraser W, Trivelpiece W, Trivelpiece S (1997) Effects of sea-ice extent and krill or salp dominance on the Antarctic food web. Nature 387:897–900

Menden-Deuer S, Lessard EJ (2000) Carbon to volume relationships for dinoflagellates, diatoms, and other protist plankton. Limnol Oceanogr 45:569–579

Menzel DW, Ryther JH (1964) The composition of particulate organic matter in the western North Atlantic. Limnol Oceanogr 9:179–186

Mines CH, Ghadouani A, Legendre P, Yan ND, Ivey GN (2013) Examining shifts in zooplankton community variability following biological invasion. Limnol Oceanogr 58:399–408

Mountford K (1980) Occurrence and predation by *Mnemiopsis leidyi* in Barnegat Bay, New Jersey. Estuar Coast Mar Sci 10:393–402

Olsen PS, Mahoney JB (2001) Phytoplankton in the Barnegat Bay–Little Egg Harbor estuarine system: species composition and picoplankton bloom development. J Coastal Res Spec Issue 32:115–143

Poulet SA, Marsot P (1978) Chemosensory grazing by marine calanoid copepods (Arthropoda: Crustacea). Science 200:1403–1405

Prowe AEF, Pahlow M, Dutkiewicz S, Follows M, Oschlies A (2012) Top-down control of marine phytoplankton diversity in a global ecosystem model. Prog Oceanogr 101: 1–13

Purcell JE (1992) Effects of predation by the scyphomedusan *Chrysaora quinquecirrha* on zooplankton populations in Chesapeake Bay, USA. Mar Ecol Prog Ser 87:65–76

Purcell JE, Cowan JH Jr (1995) Predation by the scypho-

medusan *Chrysaora quinquecirrha* on *Mnemiopsis leidyi* ctenophores. Mar Ecol Prog Ser 129:63−70

Purcell JE, White JR, Roman MR (1994) Predation by gelatinous zooplankton and resource limitation as potential controls of *Acartia tonsa* copepod populations in Chesapeake Bay. Limnol Oceanogr 39:263−278

Purcell JE, Shiganova TA, Decker MB, Houde ED (2001) The ctenophore *Mnemiopsis* in native and exotic habitats: U.S. estuaries *versus* the Black Sea basin. Hydrobiologia 451:145−176

Redfield A, Ketchum B, Richards F (1963) The influence of organisms on the composition of sea-water. In: Hill MN (ed) The sea, Vol 2. Harvard University Press, Cambridge, MA, p 26−77

Reid K, Croxall JP (2001) Environmental response of upper trophic-level predators reveals a system change in an Antarctic marine ecosystem. Proc R Soc Lond B Biol Sci 268:377−384

Riley GA (1965) A mathematical model of regional variations in plankton. Limnol Oceanogr 10:202−215

Sandine PH (1984) Zooplankton. In: Kennish MJ, Lutz RA (eds) Lecture notes on coastal and estuarine studies 6: ecology of Barnegat Bay, New Jersey. Springer-Verlag, New York, NY, p 95−134

Schneider G, Behrends G (1998) Top-down control in a neritic plankton system by *Aurelia aurita* medusae — a summary. Ophelia 48:71−82

Sommer U (2008) Trophic cascades in marine and freshwater plankton. Int Rev Hydrobiol 93:506−516

Strickland JD (1960) Measuring the production of marine phytoplankton. J Fish Res Board Can 122:1−172

Suchman CL, Sullivan BK (1998) Vulnerability of the copepod *Acartia tonsa* to predation by the scyphomedusa *Chrysaora quinquecirrha*: effect of prey size and behavior. Mar Biol 132:237−245

Turner JT (2004) The importance of small planktonic copepods and their roles in pelagic marine food webs. Zool Stud 43:255−266

Verity PG, Robertson CY, Tronzo CR, Andrews MG, Nelson JR, Sieracki ME (1992) Relationships between cell volume and the carbon and nitrogen content of marine photosynthetic nanoplankton. Limnol Oceanogr 37: 1434−1446

Visser AW, Fiksen Ø (2013) Optimal foraging in marine ecosystem models: selectivity, profitability and switching. Mar Ecol Prog Ser 473:91−101

Wieben CM, Baker RJ (2009) Contributions of nitrogen to the Barnegat Bay–Little Egg Harbor Estuary: updated loading estimates. Barnegat Bay National Estuary Program Report Prepared for Inclusion in a Future BBNEP State of the Bay Technical Report. Available at http:// bbp.ocean.edu/Reports/USGS_NLoadUpdate_Final.pdf

Wirtz KW (2012) Who is eating whom? Morphology and feeding type determine the size relation between planktonic predators and their ideal prey. Mar Ecol Prog Ser 445:1−12